Published in final edited form as:
Cell. 2014 October 9; 159(2): 318–332. doi:10.1016/j.cell.2014.09.035.

Discovery of a class of endogenous mammalian lipids with anti-diabetic and anti-inflammatory effects

Mark M. Yore[*,a], **Ismail Syed**[*,a], **Pedro M. Moraes-Vieira**[*], **Tejia Zhang**[^], **Mark A. Herman**[*], **Edwin Homan**[^], **Rajesh T. Patel**[+], **Jennifer Lee**[*], **Shili Chen**[^], **Odile D. Peroni**[*], **Abha Dhaneshwar**[*], **Ann Hammarstedt**[†], **Ulf Smith**[†], **Timothy E. McGraw**[+], **Alan Saghatelian**[^,b], and **Barbara B. Kahn**[*,b]

[*]Division of Endocrinology, Diabetes & Metabolism, Department of Medicine, Beth Israel. Deaconess Medical Center and Harvard Medical School, Boston, MA 02215

[+]Department of Biochemistry, Weill Cornell Medical College, New York, NY 10065

[^]Department of Chemistry and Chemical Biology, Harvard University, Cambridge, MA 02138

[†]Department of Molecular and Clinical Medicine, the Sahlgrenska Academy, University of Gothenburg, Gothenburg, Sweden

Summary

Increased adipose tissue lipogenesis is associated with enhanced insulin sensitivity. Mice overexpressing the Glut4 glucose transporter in adipocytes have elevated lipogenesis and increased glucose tolerance despite being obese with elevated circulating fatty acids. Lipidomic analysis of adipose tissue revealed the existence of branched fatty acid esters of hydroxy fatty acids (FAHFAs) that were elevated 16–18-fold in these mice. FAHFA isomers differ by the branched ester position on the hydroxy fatty acid (e.g. palmitic-acid-9-hydroxy-stearic acid, 9-PAHSA). PAHSAs are synthesized in vivo and regulated by fasting and high fat feeding. PAHSA levels correlate highly with insulin sensitivity and are reduced in adipose tissue and serum of insulin-resistant humans. PAHSA administration in mice lowers ambient glycemia and improves

Address correspondence to Barbara B. Kahn at bkahn@bidmc.harvard.edu or Alan Saghatelian at asaghatelian@salk.edu.
[a,b]same letter denotes equal contribution.
Current address for Tejia Zhang, Shili Chen and Alan Saghatelian: Salk Institute for Biological Studies, Torrey Pines Road, La Jolla, CA 92037.

Supplemental information
Supplemental Information includes: Extended experimental procedures, 4 figures, and 3 tables.

Author Contributions
M.M.Y. and I.S. conceived of, designed, performed, and interpreted experiments and made figures. P.M.M.V. designed, performed and interpreted the immunology experiments and made the figures. M.A.H. conceived of the untargeted lipidomics experiment and E.A.H. and M.A.H. designed and performed the untargeted lipidomics experiment. E.A.H. designed, performed and interpreted the data from the structure elucidation studies. E.A.H. and A.S. designed and performed chemical synthesis of the lipids. T.Z., I.S., E.A.H. and S.C. developed and applied new targeted lipidomics methods. J.L., A.D., O.D.P. assisted with animal studies. B.B.K., I.S., U.S., and A.H. designed, performed and interpreted the data from human studies. R.T.P, T.E.M. designed and performed Glut4 translocation assays. B.B.K. and A.S. conceived of, designed and supervised the experimental plan and interpreted experiments. B.B.K., A.S., M.M.Y. and I.S. wrote the manuscript. M.A.H., P.M.M.V., O.D.P., T.E.M., and J.L. edited the manuscript.

glucose tolerance while stimulating GLP-1 and insulin secretion. PAHSAs also reduce adipose tissue inflammation. In adipocytes, PAHSAs signal through GPR-120 to enhance insulin-stimulated glucose uptake. Thus, FAHFAs are endogenous lipids with the potential to treat type 2 diabetes.

Introduction

Obesity and type 2 diabetes (T2D) are at epidemic proportions worldwide (Hu, 2011). The major pathogenic factors underlying T2D are resistance to insulin action in peripheral tissues and dysregulated insulin secretion. The Glut4 glucose transporter is the major insulin-regulated glucose transporter and mediates glucose uptake into skeletal muscle, heart, and adipocytes in response to rising insulin after a meal (Shepherd and Kahn, 1999). In humans and rodents with obesity or T2D, Glut4 is downregulated selectively in adipose tissue (AT) and not in muscle (Shepherd and Kahn, 1999). This alters AT biology leading to systemic insulin resistance (Abel et al., 2001). Glut4 knockdown selectively in adipocytes in mice results in insulin resistance and increased T2D risk (Abel et al., 2001), whereas adipose-selective overexpression of Glut4 (AG4OX) lowers fasting glycemia and enhances glucose tolerance (Carvalho et al., 2005; Shepherd et al., 1993). These effects in AG4OX mice are mediated by glucose-dependent induction of lipogenesis in AT driven by ChREBP (Herman et al., 2012), a transcription factor that regulates both glycolysis and lipogenesis (Iizuka et al., 2004; Ma et al., 2005). ChREBP knockout in AG4OX mice completely reverses the enhanced glucose tolerance (Herman et al., 2012). Expression of ChREBP and lipogenic genes in AT is highly associated with insulin sensitivity in humans and rodents (Herman et al., 2012; Roberts et al., 2009) and increased *de novo* lipogenesis in AT has favorable metabolic effects including potentially increasing longevity (Bruss et al., 2010).

Elevated circulating fatty acids are generally associated with insulin resistance and glucose intolerance (Boden and Shulman, 2002). However, certain fatty acids such as dietary omega-3 fatty acids (Oh et al., 2010; Virtanen et al., 2014) and the endogenously produced palmitoleate (Cao et al., 2008) have favorable metabolic effects. Furthermore, large epidemiological studies show that an increased ratio of unsaturated to saturated fatty acids in serum triacylglycerols is associated with a reduced risk of T2D (Rhee et al., 2011; Riserus et al., 2009). Similarly, an increased ratio of monounsaturated to saturated fatty acids in the liver is associated with insulin sensitivity even with extensive hepatic steatosis (Benhamed et al., 2012). AG4OX mice have elevated circulating fatty acids and increased adiposity, yet have lower fasting glycemia and profoundly enhanced glucose tolerance compared to controls (Carvalho et al., 2005; Herman et al., 2012; Shepherd et al., 1993). This raised the possibility that enhanced AT lipogenesis in response to Glut4 overexpression might drive the production of lipids which have favorable metabolic effects. Since Glut4 (Carvalho et al., 2005; Shepherd and Kahn, 1999) and ChREBP (Herman et al., 2012) expression are downregulated in AT in insulin-resistant humans and rodents, the production of these metabolically favorable lipids may be low in these states. To test these hypotheses, we performed lipidomic analysis of AT from wildtype (WT) and AG4OX mice.

Identification of a class of Glut4-regulated lipids

Using a quantitative mass spectrometry (MS) lipidomics platform (Saghatelian et al., 2004), we detected more than 1400 ions in AT, 6% of which had a 2–4-fold difference between AG4OX and WT mice. A cluster of ions in AG4OX AT was elevated ≥16-fold (Fig 1A). Determining the "exact mass" of these ions enabled us to calculate their molecular formulas as $C_{32}H_{61}O_4$ (509.4575), $C_{34}H_{63}O_4$ (535.4732), $C_{34}H_{65}O_4$ (537.4888) and $C_{36}H_{67}O_4$ (563.5045). These formulas all contain a unique signature of 4 oxygen atoms indicating that these ions are members of a single lipid class. These formulas do not correspond to any known metabolite in the Metlin (Smith et al., 2005) and Lipid Maps (Sud et al., 2007) metabolite databases. We hypothesized these lipids might contribute to glucose-insulin homeostasis because of their abundance in AG4OX mice, in which improved glucose tolerance depends on enhanced AT lipogenesis (Herman et al., 2012). Therefore, we proceeded to determine the molecular structures and biologic effects of these lipids.

The mass differences among these ions suggested they contain fatty acids. Fragmentation of the 537 ion generated several product ions with masses of 255, 281 and 299 (Fig 1B), which correspond to palmitic acid (PA), octadecenoic acid, and hydroxy-stearic acid (HSA), respectively. The molecular formula of the 537 ion ($C_{34}H_{65}O_4$) does not contain any double bonds. This indicates that octadecenoic acid, which contains a double bond, results from fragmentation in the MS and is not part of the natural metabolite. Based on the chemical formula and the fact that this metabolite ionized only in the negative mode, the most reasonable structure for the 537 ion is an ester that combines PA and HSA to yield Palmitic Acid-Hydroxy Stearic Acid (PAHSA) (Fig 1B–C). Based on this structural model and the masses detected for the other elevated ions, their structures are: Palmitic Acid-Hydroxy Palmitic Acid (PAHPA, m/z 509), Oleic Acid-Hydroxy Stearic Acid (OAHSA, m/z 563), and the 535 ion is a mixture of PalmitOleic Acid-Hydroxy Stearic Acid (POHSA) and Oleic Acid-Hydroxy Palmitic Acid (OAHPA) (Fig 1C). We refer to this class of natural-occurring lipids as Fatty Acid-Hydroxy Fatty Acids (Fig 1C–D), abbreviated as FAHFAs. An additional ion, detected in positive ionization mode, was also upregulated in AG4OX AT (Fig 1A) but the molecular formula indicated it is not a FAHFA and therefore we did not characterize it further.

Using a targeted MS approach, we identified 16 FAHFA family members in mouse serum that consisted of 4 fatty acids and 4 hydroxy-fatty acids in different combinations (Fig 1D). FAHFAs with PO, PA or OA as the fatty acid moiety and HPA or HSA as the hydroxy-fatty acid moiety were most highly increased in AG4OX compared to WT mice (Fig 1D). Because PAHSAs were the most highly upregulated family member in AT of AG4OX (Fig 1A), we investigated their biologic effects.

Tissue distribution of total PAHSAs in WT and AG4OX mice and regulation by ChREBP

Targeted MS revealed PAHSAs in all tissues analyzed. In WT mice, total PAHSA levels are highest in brown adipose tissue (BAT) followed by subcutaneous (SQ) white adipose tissue (WAT), perigonadal (PG) WAT and liver (Fig 1E). Total PAHSA levels are very low in

heart and gastrocnemius muscle (data not shown). In WT serum, total PAHSA levels are ~7nM (Fig 1E). In AG4OX mice, total PAHSA levels are 16–18 fold elevated in SQ and PG WAT, 3-fold in BAT and ~2-fold in serum compared to WT mice (Fig 1E). In contrast, PAHSA levels in liver of AG4OX mice are ~30% lower than WT. Thus, Glut4 overexpression in AT results in broad systemic regulation of PAHSAs with tissue-specific alterations. Furthermore, PAHSA levels vary >7-fold among tissues in WT mice (Fig 1E).

Because ChREBP regulates AT lipogenesis in AG4OX, we tested whether ChREBP regulates PAHSA levels *in vivo.* ChREBP knockout in normal mice reduces total PAHSA levels ~75% in PG- and SQ-WAT with no change in serum (Fig 1F). Knocking out ChREBP in AG4OX completely reverses the marked elevation in PAHSA levels in PG- and SQ-WAT and serum.

Tissue distribution of specific PAHSA isomers and regulation in WT and AG4OX mice

We observed multiple peaks in the chromatograms which correspond to different PAHSA isomers with the ester connected to a different carbon of the hydroxy-fatty acid resulting in a branched lipid. Fragmentation of PAHSAs from AT using high collisional energy tandem MS (Moe et al., 2004) produced two ions at 127 and 155 (Fig 1B) indicating that the ester is at the 9^{th} carbon of the HSA (Fig 1C). We refer to this isomer as 9-PAHSA which was confirmed by chemical synthesis and co-elution with ^{13}C-9-PAHSA (Fig 2A). We also discovered PAHSAs with branched esters at carbons 5, 7, 8, 10, 11, 12 and 13 verified by comparison to synthetic standards (Fig 2A). Thus, there are at least 8 PAHSA isomers. We achieved complete separation of all isomers except 13- and 12-PAHSA (Fig 2A), which we quantify together in all data sets.

We sought to determine which PAHSA isomers are upregulated in WAT and serum of AG4OX mice as an initial clue to which ones may have biologic activities that could affect glucose homeostasis. In WT serum, 13/12-, 11-, 10-, 9-, and 5-PAHSA are present at 0.4–2.5 nM which is the range for signaling lipids such as prostacyclins, prostaglandins, steroids and endocannabinoids. In WT WAT and BAT, 9-PAHSA is the most abundant isomer (Fig 2B). 13/12-, 11- and 10-PAHSA are present at 20–30% of 9-PAHSA levels and 8-, 7-, and 5-PAHSA are present at substantially lower concentrations (Fig 2B). Surprisingly, liver which is also a lipogenic tissue, has only 13/12- and 9-PAHSAs (Fig 2B). In AG4OX mice, all PAHSA isomers are elevated in serum, SQ and PG WAT and BAT with 9-PAHSA being the most highly upregulated. In contrast, in AG4OX liver, PAHSA isomers are reduced compared to WT. These data reveal that individual PAHSA isomers are coordinately upregulated in AG4OX WAT and BAT which may result from the effect of increased Glut4 to induce ChREBP and lipogenesis in these tissues (Herman et al., 2012; Tozzo et al., 1995). However, PAHSAs are reduced in AG4OX liver indicating tissue-specific mechanisms for regulating uptake, synthesis, degradation or release.

This is further indicated by the tissue distribution of specific PAHSA isomers in WT mice. 13/12- and 9-PAHSAs are present in all WT tissues examined (Fig 2C). 9-PAHSA is more

abundant in AT than liver while 13/12-PAHSA is not. In contrast to 13/12- and 9-PAHSA, 5-PAHSA is restricted to AT, kidney and serum (Fig 2C).

Physiologic regulation of PAHSAs with fasting

We examined PAHSA regulation with fasting (Fig 2D). In the fed state, total PAHSA levels are highest in BAT, slightly lower in SQ and PG WAT and substantially lower in liver, pancreas and kidney (Fig 2D). Fasting increases PAHSAs 2–3-fold in WAT and kidney and 65% in pancreas but does not alter the levels in BAT, liver or serum (Fig 2D). Hence, PAHSAs undergo tissue-specific regulation with fasting (Fig 2D). The fasting-induced increase in PAHSAs in WAT is surprising since one would expect synthesis to be lower due to reduced lipogenesis and ChREBP with fasting. Indeed, in spite of elevated PAHSA levels, biosynthetic activity (described below) was not increased in WAT from fasted mice (not shown). This may reflect inhibition of degradation or release. To better understand the mechanism, we determined fasting effects on PAHSA levels in AG4OX mice. Fasting further elevated PAHSAs in WAT but not in BAT or serum (Fig S1). Since PAHSA levels in AG4OX WAT are regulated by ChREBP-driven lipogenesis (Fig 1E) and lipogenesis is not increased with fasting, these data demonstrate an additional level of regulation and support the possibility that fasting inhibits PAHSA degradation or release.

We also investigated regulation of individual PAHSA isomers with fasting (Fig 2E). Although total PAHSA levels are unchanged in serum of fasted mice (Fig 2D), specific isomers (10-, 9- and 5-PAHSA) are modestly decreased (Fig 2E). In SQ and PG WAT, most of the isomers (13/12-, 11-, 10-, 9- and 8-PAHSA) including the more abundant ones are increased with fasting while 7- and 5-PAHSA are unchanged (Fig 2E). Fasting had no effect on any PAHSA isomer in BAT or liver while all isomers were upregulated in kidney. In pancreas, 11- and 9-PAHSA are increased with fasting while 13/12- and 7-PAHSA are unchanged. Thus, PAHSA isomer levels undergo tissue-specific and isomer-specific regulation with fasting (Fig 2E). The abundance of different PAHSA isomers in the fasted state differs by 60-fold in a given tissue (compare 9- with 5-PAHSA in SQ WAT) (Fig 2E). These results suggest that fasting regulates pathways involved in synthesis, degradation and/or release of specific PAHSA isomers in a tissue- and isomer-specific manner.

Regulation of PAHSAs in obesity and insulin resistance

We investigated PAHSA levels in insulin-resistant mice with high fat diet (HFD)-induced obesity (Fig 3A). After 9 weeks of HFD, mice were obese and diabetic (determined by GTT) (Fig S2A). HFD had differential effects on specific PAHSA isomers. 5- and 13/12-PAHSAs were downregulated in HFD mice in serum, PG and SQ WAT and BAT (Fig 3A) although the difference did not reach significance for 13/12-PAHSA in PG WAT. Strikingly, 10-, 9-, 8-, and 7-PAHSA were increased in PG WAT of HFD-fed mice. Most of these isomers were decreased in SQ WAT and BAT and unchanged in serum (Fig 3A). Total lipid ion signal measured in SQ WAT was unchanged between Chow and HFD fed mice (Fig S2B). 13/12- and 9-PAHSA were also decreased in liver (Fig 3A). These studies demonstrate: 1) 5-PAHSA and 13/12-PAHSA are consistently reduced in AT depots with HFD while other PAHSA isomers have opposite regulation among the depots (PG WAT versus SQ WAT and

BAT) (Fig 3A); and 2) Only 2 of the 5 isomers in serum are reduced with HFD (Fig 3A). Thus, PAHSAs undergo isomer-specific and tissue-specific regulation under insulin-resistant conditions in WT mice.

PAHSAs are present in food

To determine whether the changes in PAHSA levels in altered metabolic states could result from differences in dietary intake, we measured PAHSA levels in rodent and human foods. In chow and HFD, we found 5 of the 7 isomers that are present in mouse AT, 13/12-, 11-, 10-, 9- and 8-PAHSA, but not 7- and 5-PAHSA. However, the relative abundance was strikingly different from AT or serum with 10-PAHSA being most abundant in both diets (Fig 3B). Levels of all these isomers were substantially lower in HFD than chow (Fig 3B). Given that PAHSAs increase in WAT during fasting (Fig 2D-E), regulation of tissue PAHSA levels does not simply reflect dietary intake. Similarly, the abundance of PAHSA isomers in serum and tissues (Fig 2C) does not correlate with predominant isomers in chow (Fig 3B), suggesting that PAHSAs present in tissues are synthesized endogenously. The fact that 5-PAHSA is not present in mouse chow or HFD (Fig 3B) but is present in WAT, BAT, kidney and serum (Fig 2A-C, E and 3A) further supports this notion. We also found PAHSAs in all human foods tested with different isomer distributions and abundance (Fig S2C).

PAHSAs are synthesized in mammalian tissues

To determine whether PAHSAs are synthesized endogenously, we investigated PAHSA biosynthesis in liver and WAT lysates of normal mice. We detected PAHSA biosynthetic activity in both tissues and it was markedly reduced by heat denaturation (Fig 3C). We also detected PAHSA biosynthesis *in vivo*. Gavage of mice with 9-hydroxy heptadecanoic acid (9-HHA), a hydroxy fatty acid not normally found in mammalian tissues resulted in synthesis of full length FAHFAs containing a 9-HHA acyl chain indicating that FAHFAs can be synthesized *in vivo* (Fig 3D).

PAHSAs are present in humans and levels are reduced with insulin resistance

To determine if PAHSAs are present in humans and are regulated in disease states, we measured PAHSA isomers in serum and SQ WAT from insulin-sensitive and insulin-resistant non-diabetic humans. Subjects were middle-aged. BMI was increased in 5 out of 6 insulin-resistant participants (table S1). Insulin resistance was demonstrated by a 61% reduction in glucose infusion rate during a euglycemic hyperinsulinemic clamp (table S1). Serum triglycerides and free fatty acids in the fasting state were not different between groups (table S1). Total PAHSA levels are reduced ~40% in serum of insulin-resistant humans (Fig 4A). In serum of both insulin-sensitive and insulin–resistant humans, 9- and 10-PAHSA are most abundant and 13/12- and 5-PAHSAs are present at ~1/5 of these concentrations (Fig 4A). In insulin-resistant people, serum levels of all PAHSAs except 9-PAHSA are reduced by 40–55% compared to insulin-sensitive people (Fig 4A). Serum concentrations of total PAHSAs and all isomers correlated remarkably strongly with insulin

sensitivity measured by clamp (Fig 4B). Serum PAHSA levels did not correlate with levels of nonesterified fatty acids or triglycerides (data not shown) suggesting that PAHSAs levels are regulated by different mechanisms.

In human SQ WAT, total PAHSAs are reduced ~70% (Fig 4C). We detected 13/12-, 11-, 10-, 9-, and 5-PAHSA isomers in these biopsies (Fig 4C). However, for technical reasons we were unable to quantify the levels of 11-PAHSA. 9-PAHSA levels were higher than all other isomers (Fig 4C) similar to mouse SQ WAT (Fig 2B, 2E and 3A). 13/12-, 10-, 9- and 5-PAHSA concentrations in SQ WAT of insulin-resistant people were 60–73% lower than in insulin-sensitive people (Fig 4C). Concentrations of total PAHSAs and of 9- and 5-PAHSA isomers in WAT correlate highly with insulin sensitivity (Fig 4D). Serum PAHSA levels correlated with WAT PAHSA levels only for 5-PAHSA (Fig 4E).

In summary, all PAHSA isomers detected are reduced in SQ WAT in insulin-resistant subjects and all but one are reduced in serum. Furthermore, PAHSA levels in serum and WAT correlate highly with whole body insulin sensitivity. These effects parallel the effects in diet-induced obese mice in which all PAHSA isomers are reduced in SQ WAT, and 13/12- and 5-PAHSA are lower in serum compared to chow-fed mice (Fig 3A). Thus, the regulation of PAHSAs and their inverse correlation with insulin resistance is conserved between mice and humans.

PAHSAs acutely improve glucose tolerance and ambient glycemia

Since levels of PAHSA isomers correlate with insulin sensitivity (Fig 4B and 4D), we tested whether administration of PAHSAs could improve glucose homeostasis in obese, diabetic mice. We selected 9-PAHSA and 5-PAHSA because: 1) 9-PAHSA was the most abundant form in WAT and BAT in WT mice (Fig 2B) and in SQ WAT of humans (Fig 4C). 2) 9-PAHSA is the most strongly upregulated in serum and WAT of insulin-sensitive AG4OX mice (Fig 2B) and was downregulated (with other isomers) in WAT of insulin-resistant humans (Fig 4C). 3) 5-PAHSA was the most consistently downregulated in all adipose depots and in serum of insulin-resistant mice (Fig 3A) and in WAT and serum of insulin-resistant humans. Oral gavage of 5-PAHSA increased serum levels 3–5-fold in mice on chow and HFD (Fig S3). As shown in figure 3A, baseline 5-PAHSA levels were 50–80% lower in HFD-fed mice compared to chow-fed mice and 5-PAHSA gavage more than restored the levels (Fig S3). The post-gavage elevation of serum 5-PAHSA levels in both chow and HFD-fed mice was similar to the elevation in serum of AG4OX mice (Fig 2B and S2). This indicated that PAHSAs are absorbed orally and this route of administration can be used to increase PAHSA concentrations for *in vivo* metabolic studies.

Acute oral administration of 5- or 9-PAHSA in insulin-resistant HFD-fed mice lowered basal glycemia at 30 minutes after PAHSA administration (Fig 5A,-30 to 0 minutes). Subsequently, glucose was administered and we observed improved glucose tolerance in PAHSA-treated mice with reduced area under the glucose excursion curve (Fig 5A). Because of the significant effect of PAHSAs on the baseline glucose levels in HFD-fed mice at 30 minutes after administration, we tested whether PAHSA action to lower baseline glycemia was sustained. 5-PAHSA or 9-PAHSA had a greater glucose-lowering effect than

vehicle treatment in HFD-fed mice also at 2.5–3 hours after administration (Fig 5B). There was no difference in plasma insulin levels at this time in PAHSA-treated compared to vehicle-treated mice (data not shown). Since no food was available during this study, calorie absorption was not a variable and the results suggest that oral PAHSA administration enhances insulin sensitivity. An insulin tolerance test showed lower glucose levels in PAHSA-treated mice compared to vehicle-treated mice for the study duration (120 min after insulin administration) which was largely because of the PAHSA effect to lower baseline glycemia (data not shown).

PAHSAs stimulate insulin and GLP-1 secretion

To determine whether enhanced insulin secretion might contribute to the PAHSA-induced improvement in glucose tolerance (Fig 5A), we tested PAHSA effects on glucose-stimulated insulin secretion (GSIS) *in vivo* in aged chow-fed mice. 5-PAHSA improved glucose tolerance (Fig 5C) concurrent with acute enhancement of insulin secretion at 5 minutes after glucose administration (Fig 5D). This may result from direct effects on insulin secretion or from stimulation of incretin secretion since GLP-1 levels were also increased in PAHSA-treated mice at 5 minutes after glucose administration (Fig 5E). Thus, PAHSAs augment the acute stimulation of GLP-1 and insulin secretion in response to glucose and these effects most likely have an important role in the enhanced glucose tolerance following a single PAHSA dose.

To determine whether the stimulation of insulin secretion is a direct effect of PAHSAs on pancreatic beta cells, we incubated islets from human donors (table S2, donors' metabolic parameters) with 5-PAHSA and measured GSIS. 5-PAHSA had no effect on insulin secretion at 2.5mM glucose but augmented the insulin secretion response at 20mM glucose (Fig 5F). These data demonstrate that 5-PAHSA directly enhances GSIS in human islets. To determine whether PAHSAs directly stimulate GLP-1 secretion, we used the enteroendocrine cell line STC-1. Both 5- and 9-PAHSA rapidly stimulated GLP-1 secretion from STC-1 cells in a dose-dependent manner (Fig 5G). The effects are similar to those with the omega-3 fatty acid, α-linolenic acid, and a synthetic GPR120 ligand (Fig 5G). Thus, the rapid effects of PAHSAs to augment GSIS may be both direct effects on pancreatic beta cells and indirect effects through stimulation of GLP-1 secretion.

PAHSAs enhance insulin-stimulated glucose transport and Glut4 translocation by activating GPR120

To further understand the mechanism(s) by which PAHSAs improve glucose homeostasis, we tested their effects on glucose transport in adipocytes. PAHSAs increased glucose transport at sub-maximal and maximal insulin concentrations (Fig 6A). Neither of the fatty acids that form the parent PAHSA structure, palmitic acid or hydroxystearic acid, alone improved insulin-stimulated glucose transport (Fig 6B). The effects of PAHSAs on insulin–stimulated glucose transport occurred with both acute (30 min) and chronic (2–6 day) treatment and at concentrations as low as 500nM (Fig S4A). PAHSAs did not alter total cellular Glut1 or Glut4 protein levels in adipocytes even after 6 days of incubation (data not shown).

Bioactive lipids can influence biology through binding to cell surface receptors such as G Protein-Coupled Receptors (GPCRs) (Hara et al., 2013). The effects of PAHSAs on GLP-1 secretion and glucose transport are consistent with possible activation of GPCRs (Hirasawa et al., 2005). To determine whether PAHSAs activate GPCRs, we screened a panel of known lipid-activated GPCRs. Both 9-PAHSA (Fig 6C) and 5-PAHSA (data not shown) dose-dependently bind to and activate GPR120 which is also activated by ω-3 fatty acids and monounsaturated fatty acids (Hirasawa et al., 2005; Oh et al., 2010). Activation of GPR120 increases glucose transport and Glut4 translocation in adipocytes (Oh et al., 2010). To test whether GPR120 mediates the effects of PAHSAs, we knocked it down >95% in adipocytes with siRNA (Fig S4B). This completely reversed the enhanced effects of PAHSAs on insulin-stimulated glucose transport (Fig 6D). These data demonstrate that GPR120 mediates the effects of PAHSAs on insulin-stimulated glucose transport.

To determine the mechanism for enhancement of glucose transport with PAHSAs we analyzed the effects on insulin-induced Glut4 translocation to the plasma membrane in adipocytes. In the absence of insulin, PAHSAs had no effect on Glut4 translocation (Fig 6F). However, PAHSAs enhanced Glut4 translocation at submaximal and maximal insulin concentrations (Fig 6E-F). These data indicate that PAHSAs augment insulin-stimulated glucose transport by enhancing Glut4 translocation. Knockdown of GPR120 in adipocytes completely blocked the effect of PAHSAs to augment insulin-stimulated Glut4 translocation (Fig 6E-F). We obtained this effect with two different GPR120 siRNAs indicating that it is a specific “on target” effect. These data together demonstrate that PAHSAs bind to and activate GPR120 (Fig 6C) which mediates the effects of PAHSAs on insulin-stimulated glucose transport and Glut4 translocation (Fig 6D-F).

PAHSAs exert anti-inflammatory effects

Fatty acids, such as ω-3 fatty acids, can elicit anti-inflammatory effects through GPR120 (Oh et al., 2010). GPR120 is expressed in bone marrow derived dendritic cells (BMDCs), which are initial antigen-presenting cells in the innate immune response. Innate immunity is activated in WAT in obesity and may contribute to the insulin-resistant state (Lumeng and Saltiel, 2011). Saturated fatty acids such as palmitic acid and pathogen-derived molecules, such as lipopolysaccharide (LPS), promote BMDC maturation by activating Toll-like receptors (TLRs) (Lumeng and Saltiel, 2011). This induces expression of pro-inflammatory cytokines, major histocompatibility complex II (MHC II) and co-stimulatory molecules (CD40, CD80 and CD86) required for antigen presentation and T-cell activation. LPS addition to BMDCs robustly increased CD80, CD86, CD40 and MHC II expression, demonstrating the expected activation of BMDCs (Fig 7A). 9-PAHSA blocked the LPS effect on BMDC activation as evidenced by inhibition of LPS-induced CD80, CD86, CD40 and MHC II expression (Fig 7A-B). Neither palmitic acid which is a component of the PAHSA molecule, nor the mono-unsaturated fatty acid, oleic acid, exerted these effects at a concentration (20 μM) (Fig S5) at which 9-PAHSA had strong anti-inflammatory effects (Fig 7B). 9-PAHSA completely blocked LPS-induced IL-12 secretion in a dose-dependent manner (Fig 7C) and substantially reduced IL-1β and TNFα at doses as low as 8 μM (Fig 7C). These data indicate that 9-PAHSA has anti-inflammatory effects.

To test whether PAHSAs exert anti-inflammatory effects *in vivo,* we measured TNFα and IL- 1β in AT macrophages (ATMs) from HFD-fed mice gavaged with 9-PAHSA or vehicle for 3 days. The percentage of ATMs expressing TNFα, IL-1β or both was elevated in HFD-fed mice compared to chow. Administration of 9-PAHSA normalized the percentage of TNFα positive ATMs and reduced the percentage of IL-1β positive and double-positive ATMs (Fig 7D). Total ATM number was not reduced due to the short treatment duration (data not shown). This demonstrates that PAHSAs have anti-inflammatory effects *in vivo.* Therefore, reduced PAHSA levels in insulin resistant states (Fig 3A and 4) could contribute to activation of the innate immune system, thus playing a role in AT inflammation and systemic insulin-resistance.

Discussion

Adipose-Glut4 levels in humans are tightly associated with insulin sensitivity and lower Glut4 levels confer increased T2D risk (Carvalho et al., 2001; Shepherd and Kahn, 1999). Adipose-specific Glut4 overexpression in mice (AG4OX) causes beneficial metabolic effects which result from enhanced ChREBP-driven *de novo* lipogenesis in adipose tissue (AT) (Herman et al., 2012; Tozzo et al., 1995). Because this occurs even in the setting of obesity and elevated serum fatty acids (Herman et al., 2012; Tozzo et al., 1995), we sought to determine whether the augmented lipogenesis in AG4OX mice leads to production of lipid species that have favorable metabolic effects. Here we report the discovery of a class of mammalian lipids characterized by a branched ester linkage between a fatty-acid and a hydroxy-fatty acid or FAHFAs. The closest reported structures are (O-acyl)-omega hydroxy-fatty acids in the eye (Butovich et al., 2009) which are not branched.

Of the 16 FAHFA family members we report here, we extensively characterized the biology of PAHSA isomers which are present in many, if not all, tissues and in serum in normal mice and in human WAT and serum (Fig 1–4). Total PAHSA levels are highest in WAT and BAT which also have the greatest number of PAHSA isomers (Fig 2). Furthermore, PAHSA levels are highly elevated in serum, WAT and BAT of AG4OX mice which are obese but have markedly enhanced glucose tolerance (Herman et al., 2012; Shepherd et al., 1993). In parallel, nearly all PAHSA isomers are higher in serum and SQ WAT of insulin-sensitive humans compared to insulin-resistant humans.

In insulin-resistant, obese mice, PAHSA isomer levels show adipose-depot-specific regulation and all PAHSA isomers are lower in SQ WAT of obese compared to lean mice (Fig 3). These results in SQ WAT are similar to those in insulin-resistant people (Fig 4). 5-PAHSA is consistently reduced in all adipose depots studied and in serum in insulin-resistant mice and humans. In insulin-resistant people, most PAHSA isomers are reduced in serum and AT and correlate highly with insulin sensitivity (Fig 4). ChREBP is required to maintain normal PAHSA levels in WT mice and elevated levels in AG4OX mice (Fig 1F). In humans, ChREBP and lipogenic enzyme expression correlate strongly with insulin-sensitivity. Thus, the reduction in PAHSAs in insulin-resistant people may be mediated by suppressed ChREBP expression.

This class of lipids has multiple effects that improve glucose-insulin homeostasis which suggests that restoring PAHSA levels in insulin-resistant people could have beneficial metabolic effects. Oral PAHSA administration in insulin-resistant mice on a HFD rapidly lowers ambient glucose and also improves glucose tolerance (Fig 5A-B). This may result, at least in part, from enhanced glucose transport since PAHSAs augment insulin-stimulated glucose transport and Glut4 translocation directly in adipocytes *in vitro* (Fig 6). In addition, PAHSAs stimulate both insulin and GLP-1 secretion (Fig 5D-G). Importantly, the effects of PAHSAs on insulin secretion are observed only under hyperglycemic conditions (Fig 5F). The enhanced GSIS *in vivo* most likely results from both direct effects on islet cells and indirect effects though GLP-1-stimulated insulin secretion.

Total PAHSA levels in tissues and serum are similar to concentrations of signaling lipids such as prostacyclins, prostaglandins, steroids and endocannabinoids. PAHSAs are signaling lipids that directly bind to and activate GPR120 in a cell-based GPCR activity assay (Fig 6C). GPR120 activation appears to explain the effects on insulin-induced Glut4 translocation and glucose uptake in adipocytes (Fig 6B-D), and may explain the effects on GLP-1 secretion and inhibition of inflammatory responses in immune cells. Thus, PAHSAs are endogenous GPR120 ligands and may also exert effects through other lipid-activated GPCRs.

PAHSAs have striking anti-inflammatory effects and largely block LPS-stimulated dendritic cell activation and cytokine production (Fig 7). Chronic, low-grade inflammation in AT plays an important role in obesity-related insulin resistance (Lumeng and Saltiel, 2011; Olefsky and Glass, 2010). Three days of PAHSA gavage in HFD-fed mice reduced the percentage of ATMs that express pro-inflammatory cytokines (Fig 7D). Therefore, anti-inflammatory effects of PAHSAs may promote insulin sensitivity and ameliorate other inflammatory diseases.

Insulin-sensitizing and anti-inflammatory effects and GLP-1 secretion are also observed with ω-3 fatty acids (Hirasawa et al., 2005; Oh et al., 2010). However, a major difference between ω-3 fatty acids and PAHSAs is that PAHSAs are synthesized endogenously as evidenced by PAHSA biosynthetic activity in adipose and liver lysates and incorporation of modified precursors into FAHFAs *in vivo* (Fig 3C–D). The potential importance of identifying an endogenous GPR120 ligand is demonstrated by the fact that loss of function mutations in GPR120 in humans promote obesity and insulin resistance (Ichimura et al., 2012). Thus, GPR120 is an important control point in the integration of anti-inflammatory and systemic insulin-sensitizing responses and is emerging as an important regulator of whole body glucose-insulin homeostasis (Mo et al., 2013). It is the subject of ongoing pre-clinical investigation for the treatment of obesity-related insulin resistance, T2D and inflammatory diseases (Mo et al., 2013; Oh et al., 2014).

Reduced PAHSA levels may contribute to diabetes risk since many PAHSA isomers are reduced in SQ WAT and serum of insulin-resistant rodents (Fig 3A) and humans (Fig 4). In humans, PAHSA levels in both serum and SQ WAT correlate highly with whole body insulin-sensitivity (Fig 4B and 4D). Thus, reduced circulating PAHSA levels may serve as a biomarker for insulin resistance and T2D risk. PAHSAs lower glycemia, improve glucose

tolerance and stimulate GLP-1 and insulin secretion in mice (Fig 5). This raises the possibility that restoring the reduced PAHSA levels in insulin-resistant humans could have therapeutic effects to prevent or ameliorate insulin resistance and T2D. The discovery of the FAHFAs is important also because their presence suggests uncharacterized biochemical pathways and enzymes that may be important in human physiology and disease. Changes in the levels of these metabolites and in their signaling pathways may provide important insights and new treatment avenues for metabolic and inflammatory diseases.

Experimental Procedures

Materials and reagents

All chemicals were purchased from Sigma-Aldrich (St. Louis, MO) unless otherwise stated.

Culture and differentiation of cells

3T3-L1 fibroblasts were cultured and differentiated as described (Norseen et al., 2012). STC-1 cells were maintained in DMEM supplemented with 10% FCS, pen/strep and maintained at 37°C and 5% CO_2.

Pancreatic islets, GSIS and GLP-1 secretion studies

Human islets from non-diabetic donors were obtained from Prodo Laboratories (Irvine, CA). GSIS studies (Kowluru et al., 2010) and GLP-1 secretion from STC-1 cells (Hirasawa et al., 2005) were performed as described.

Generation and treatment of bone marrow-derived dendritic cells (BMDCs)

BMDCs were generated as described (Moraes-Vieira et al., 2014). Cells were incubated with 9-PAHSA 10 min prior to LPS (100 ng/mL) stimulation. CD11c, MHC II, CD40, CD80 and CD86 (all Biolegend) were detected by flow cytometry as described (Moraes-Vieira et al., 2014). Cytokine levels were measured by ELISA (Biolegend).

9-PAHSA biosynthetic activity assay

Liver and PG-WAT tissue was Dounce homogenized in buffer A (10mM Tris-HCL pH 7.4, 250mM Sucrose containing protease inhibiters (Roche)). Lysates were centrifuged at 1200g to remove incompletely lysed cells and debris. Lysates were then adjusted to 1mg/ml protein and 100µl was incubated with 100µM palmitoyl-CoA and 100µM 9-hydroxy stearic acid (PAHSA substrates) for 2h at 37°C. Control samples were heat denatured by boiling for 10 minutes prior to incubation with PAHSA substrates. After 2h the reaction was stopped by the addition of 300ul cold buffer A followed by 400ul of methanol (MeOH) and 800ul of chloroform. Samples were vortexed and centrifuged at 1200g for 5 minutes. 9-PAHSA levels in the organic layer were measured by LC-MS.

FAHFA synthesis *in vivo*

2h post food removal C57B6/J mice were gavaged with 25mg/Kg of 9-hydroxy heptadecanoic acid or vehicle. 3h later mice were sacrificed and serum was collected. Serum lipids were extracted and 9-PAHHA levels measured by LC-MS.

Animal studies and measurement of metabolic parameters

Female AG4OX mice and WT FVB littermate controls (Shepherd et al., 1993) at 8–14 weeks old were used for FAHFA tissue distribution and regulation with fasting and HFD studies. ChREBP-KO, ChREBP-KO/AG4OX and control females (Herman et al., 2012) were used at 16–18 weeks old. Mice were fed on chow (Lab Diet, 5008) or HFD (Harlan Teklad, TD.93075) for 9 weeks (female FVB) or 42–52 weeks (male C57BL6/J). OGTT's were performed as described (Moraes-Vieira et al., 2014) after 5h food removal.

Anti-inflammatory effects of 9-PAHSA *in vivo*

Male C57BL6/J mice on chow or HFD described above were gavaged once a day for 3 days with 30 mg/kg (chow) or 45 mg/kg (HFD) of 9-PAHSA or an equivalent volume of vehicle. On the 4^{th} day PG stromal vascular fraction (SVF) cells were harvested and cultured for 5 hours with ionomycin, PMA and brefeldin at 37°C and the intracellular cytokine content was measured in gated $CD45^+$, $CD11b^+$ and $F4/80^+$ cells as described (Moraes-Vieira et al., 2014).

Human studies

Hyperinsulinemic-euglycemic clamp was performed in 13 non-diabetic subjects. SQ WAT biopsies were obtained from the peri-umbilical, abdominal region after an overnight fast.

Lipid extraction

Lipid extraction was performed as described (Bligh and Dyer, 1959; Saghatelian et al., 2004). Tissues (60–150 mg) were Dounce homogenized on ice in a mixture of 1.5ml MeOH, 1.5ml chloroform and 3ml citric acid buffer. PAHSA standards were added to chloroform prior to extraction. The resulting mixture was centrifuged and the organic phase containing extracted lipids was dried under N_2 and stored at −80°C prior to solid phase extraction.

Lipidomic analysis

Lipidomic analysis was performed using an Agilent 6220 ESI-TOF fitted with an electrospray ionization source with a capillary voltage of 3500kV and fragmentor voltage of 100V. A Gemini C18 reversed phase column (Phenomenex) and a C18 reversed phase guard column (Western Analytical) was used for LC–MS analysis in negative mode. In positive mode, a Luna C5 reversed phase column (Phenomenex) was used together with a C4 reversed phase guard column (Western Analytical). Drying gas temperature was 350°C, flow rate 10L/min and nebulizer pressure 45psi. Untargeted data were collected using an *m/z* of 100–1500.

Synthesis of PAHSAs and PAHSA standards

Detailed information on synthesis of PAHSAs and PAHSA standards is outlined in the SI.

Targeted LC/MS analysis of FAHFAs

FAHFAs were measured on an Agilent 6410 Triple Quad LC/MS *via* Multiple Reaction Monitoring in negative ionization mode. Extracted and fractionated samples were reconstituted in 25μL MeOH, 10μL was injected for analysis. A Luna C18(2) (Phenomenex)

column was used with an in-line filter (Phenomenex). Distinct PAHSA species were resolved *via* isocratic flow at 0.2 mL/min for 120 min using 93:7 MeOH:H_2O with 5mM ammonium acetate and 0.01% ammonium hydroxide as solvent. Transitions for endogenous PAHSAs were m/z 537.5 → m/z 255.2 (CE = 30 V), m/z 537.5 → m/z 281.2 (CE = 25 V) and m/z 537.5 → m/z 299.3 (CE = 23 V), and the transition for ^{13}C-9-PAHSA was m/z 553.5 → m/z 271.3 (CE = 30 V), all FAHFA transitions are listed in SI. Structural characterization of the FAHFAs by MS/MS was carried out on an Agilent 6510 quadrupole-time of flight MS.

Data analysis

All values are means±s.e.m. Differences between groups were assessed using unpaired two-tailed Student's t-tests and/or ANOVA with Fisher's LSD multiple comparisons as specified in figure legends. All statistical analyses were performed with GraphPad Prism 5.

Supplementary Material

Refer to Web version on PubMed Central for supplementary material.

Acknowledgments

We thank Dr. Thue Schwartz for stimulating discussions; Drs. Anna Greka and Dequan Tian for performing functional assays; Pratik Aryal, Marlee Jackson, Kerry Wellenstein and Peter Dwyer for technical assistance; and Dr. Doug Hanahan for the STC1 cells. Supported by grants from the NIH R37DK43051 and P30 DK57521 (BBK); R01 DK098002 (BBK & TEM); a grant from the JPB foundation (BBK). Searle Scholars Award, Burroughs Welcome Fund CABS, and Sloan Foundation Fellowship (AS); Harvard Training Program in Nutrition and Metabolism, 2T32HD052961–06A1 (MMY); 5T32DK007516–29 (BBK, MMY & JL); K08 DK076726 (MAH); P30 DK046200 (MAH).

References

Abel ED, Peroni O, Kim JK, Kim YB, Boss O, Hadro E, Minnemann T, Shulman GI, Kahn BB. Adipose-selective targeting of the GLUT4 gene impairs insulin action in muscle and liver. Nature. 2001; 409:729–733. [PubMed: 11217863]

Benhamed F, Denechaud PD, Lemoine M, Robichon C, Moldes M, Bertrand-Michel J, Ratziu V, Serfaty L, Housset C, Capeau J, et al. The lipogenic transcription factor ChREBP dissociates hepatic steatosis from insulin resistance in mice and humans. J Clin Invest. 2012; 122:2176–2194. [PubMed: 22546860]

Bligh EG, Dyer WJ. A RAPID METHOD OF TOTAL LIPID EXTRACTION AND PURIFICATION. Canadian Journal of Biochemistry and Physiology. 1959; 37:911–917. [PubMed: 13671378]

Boden G, Shulman GI. Free fatty acids in obesity and type 2 diabetes: defining their role in the development of insulin resistance and beta-cell dysfunction. Eur J Clin Invest. 2002; 32(Suppl 3): 14–23. [PubMed: 12028371]

Bruss MD, Khambatta CF, Ruby MA, Aggarwal I, Hellerstein MK. Calorie restriction increases fatty acid synthesis and whole body fat oxidation rates. Am J Physiol Endocrinol Metab. 2010; 298:E108–116. [PubMed: 19887594]

Butovich IA, Wojtowicz JC, Molai M. Human tear film and meibum. Very long chain wax esters and (O-acyl)-omega-hydroxy fatty acids of meibum. Journal of lipid research. 2009; 50:2471–2485. [PubMed: 19535818]

Cao H, Gerhold K, Mayers JR, Wiest MM, Watkins SM, Hotamisligil GS. Identification of a lipokine, a lipid hormone linking adipose tissue to systemic metabolism. Cell. 2008; 134:933–944. [PubMed: 18805087]

Carvalho E, Jansson PA, Nagaev I, Wenthzel AM, Smith U. Insulin resistance with low cellular IRS-1 expression is also associated with low GLUT4 expression and impaired insulin-stimulated glucose transport. FASEB J. 2001; 15:1101–1103. [PubMed: 11292681]

Carvalho E, Kotani K, Peroni OD, Kahn BB. Adipose-specific overexpression of GLUT4 reverses insulin resistance and diabetes in mice lacking GLUT4 selectively in muscle. Am J Physiol Endocrinol Metab. 2005; 289:E551–561. [PubMed: 15928024]

Hara T, Kimura I, Inoue D, Ichimura A, Hirasawa A. Free fatty acid receptors and their role in regulation of energy metabolism. Rev Physiol Biochem Pharmacol. 2013; 164:77–116. [PubMed: 23625068]

Herman MA, Peroni OD, Villoria J, Schon MR, Abumrad NA, Bluher M, Klein S, Kahn BB. A novel ChREBP isoform in adipose tissue regulates systemic glucose metabolism. Nature. 2012; 484:333–338. [PubMed: 22466288]

Hirasawa A, Tsumaya K, Awaji T, Katsuma S, Adachi T, Yamada M, Sugimoto Y, Miyazaki S, Tsujimoto G. Free fatty acids regulate gut incretin glucagon-like peptide-1 secretion through GPR120. Nat Med. 2005; 11:90–94. [PubMed: 15619630]

Hu FB. Globalization of diabetes: the role of diet, lifestyle, and genes. Diabetes Care. 2011; 34:1249–1257. [PubMed: 21617109]

Ichimura A, Hirasawa A, Poulain-Godefroy O, Bonnefond A, Hara T, Yengo L, Kimura I, Leloire A, Liu N, Iida K, et al. Dysfunction of lipid sensor GPR120 leads to obesity in both mouse and human. Nature. 2012; 483:350–354. [PubMed: 22343897]

Iizuka K, Bruick RK, Liang G, Horton JD, Uyeda K. Deficiency of carbohydrate response element-binding protein (ChREBP) reduces lipogenesis as well as glycolysis. Proc Natl Acad Sci U S A. 2004; 101:7281–7286. [PubMed: 15118080]

Lumeng CN, Saltiel AR. Inflammatory links between obesity and metabolic disease. J Clin Invest. 2011; 121:2111–2117. [PubMed: 21633179]

Ma L, Tsatsos NG, Towle HC. Direct role of ChREBP.Mlx in regulating hepatic glucose-responsive genes. J Biol Chem. 2005; 280:12019–12027. [PubMed: 15664996]

Mo XL, Wei HK, Peng J, Tao YX. Free fatty acid receptor GPR120 and pathogenesis of obesity and type 2 diabetes mellitus. Prog Mol Biol Transl Sci. 2013; 114:251–276. [PubMed: 23317787]

Moe MK, Strøm MB, Jensen E, Claeys M. Negative electrospray ionization low-energy tandem mass spectrometry of hydroxylated fatty acids: a mechanistic study. Rapid communications in mass spectrometry. 2004; 18:1731–1740. [PubMed: 15282772]

Moraes-Vieira PM, Yore MM, Dwyer PM, Syed I, Aryal P, Kahn BB. RBP4 activates antigen-presenting cells leading to adipose tissue inflammation and systemic insulin resistance. Cell Metabolism. 2014; 19:512–526. [PubMed: 24606904]

Norseen J, Hosooka T, Hammarstedt A, Yore MM, Kant S, Aryal P, Kiernan UA, Phillips DA, Maruyama H, Kraus BJ, et al. Retinol-binding protein 4 inhibits insulin signaling in adipocytes by inducing proinflammatory cytokines in macrophages through a c-Jun N-terminal kinase- and toll-like receptor 4-dependent and retinol-independent mechanism. Mol Cell Biol. 2012; 32:2010–2019. [PubMed: 22431523]

Oh DY, Talukdar S, Bae EJ, Imamura T, Morinaga H, Fan W, Li P, Lu WJ, Watkins SM, Olefsky JM. GPR120 is an omega-3 fatty acid receptor mediating potent anti-inflammatory and insulin-sensitizing effects. Cell. 2010; 142:687–698. [PubMed: 20813258]

Oh DY, Walenta E, Akiyama TE, Lagakos WS, Lackey D, Pessentheiner AR, Sasik R, Hah N, Chi TJ, Cox JM, et al. A Gpr120-selective agonist improves insulin resistance and chronic inflammation in obese mice. Nat Med. 2014

Olefsky JM, Glass CK. Macrophages, inflammation, and insulin resistance. Annu Rev Physiol. 2010; 72:219–246. [PubMed: 20148674]

Rhee EP, Cheng S, Larson MG, Walford GA, Lewis GD, McCabe E, Yang E, Farrell L, Fox CS, O'Donnell CJ, et al. Lipid profiling identifies a triacylglycerol signature of insulin resistance and improves diabetes prediction in humans. J Clin Invest. 2011; 121:1402–1411. [PubMed: 21403394]

Riserus U, Willett WC, Hu FB. Dietary fats and prevention of type 2 diabetes. Prog Lipid Res. 2009; 48:44–51. [PubMed: 19032965]

Roberts R, Hodson L, Dennis AL, Neville MJ, Humphreys SM, Harnden KE, Micklem KJ, Frayn KN. Markers of de novo lipogenesis in adipose tissue: associations with small adipocytes and insulin sensitivity in humans. Diabetologia. 2009; 52:882–890. [PubMed: 19252892]

Saghatelian A, Trauger SA, Want EJ, Hawkins EG, Siuzdak G, Cravatt BF. Assignment of Endogenous Substrates to Enzymes by Global Metabolite Profiling†. Biochemistry. 2004; 43:14332–14339. [PubMed: 15533037]

Shepherd PR, Gnudi L, Tozzo E, Yang H, Leach F, Kahn BB. Adipose cell hyperplasia and enhanced glucose disposal in transgenic mice overexpressing GLUT4 selectively in adipose tissue. J Biol Chem. 1993; 268:22243–22246. [PubMed: 8226728]

Shepherd PR, Kahn BB. Glucose transporters and insulin action--implications for insulin resistance and diabetes mellitus. N Engl J Med. 1999; 341:248–257. [PubMed: 10413738]

Smith CA, O'Maille G, Want EJ, Qin C, Trauger SA, Brandon TR, Custodio DE, Abagyan R, Siuzdak G. METLIN: a metabolite mass spectral database. Ther Drug Monit. 2005; 27:747–751. [PubMed: 16404815]

Sud M, Fahy E, Cotter D, Brown A, Dennis EA, Glass CK, Merrill AH Jr, Murphy RC, Raetz CR, Russell DW, et al. LMSD: LIPID MAPS structure database. Nucleic Acids Res. 2007; 35:D527–532. [PubMed: 17098933]

Tozzo E, Shepherd PR, Gnudi L, Kahn BB. Transgenic GLUT-4 overexpression in fat enhances glucose metabolism: preferential effect on fatty acid synthesis. Am J Physiol. 1995; 268:E956–964. [PubMed: 7762651]

Virtanen JK, Mursu J, Voutilainen S, Uusitupa M, Tuomainen TP. Serum omega-3 polyunsaturated fatty acids and risk of incident type 2 diabetes in men: the Kuopio Ischemic Heart Disease Risk Factor study. Diabetes Care. 2014; 37:189–196. [PubMed: 24026545]

Highlights

- Lipidomics identifies bioactive fatty acid esters of hydroxy fatty acids (FAHFAs)
- FAHFAs are low in insulin-resistant humans and correlate with insulin sensitivity
- These lipids improve insulin secretion and glucose tolerance in mice
- FAHFAs block inflammatory cytokine production and reduce adipose inflammation

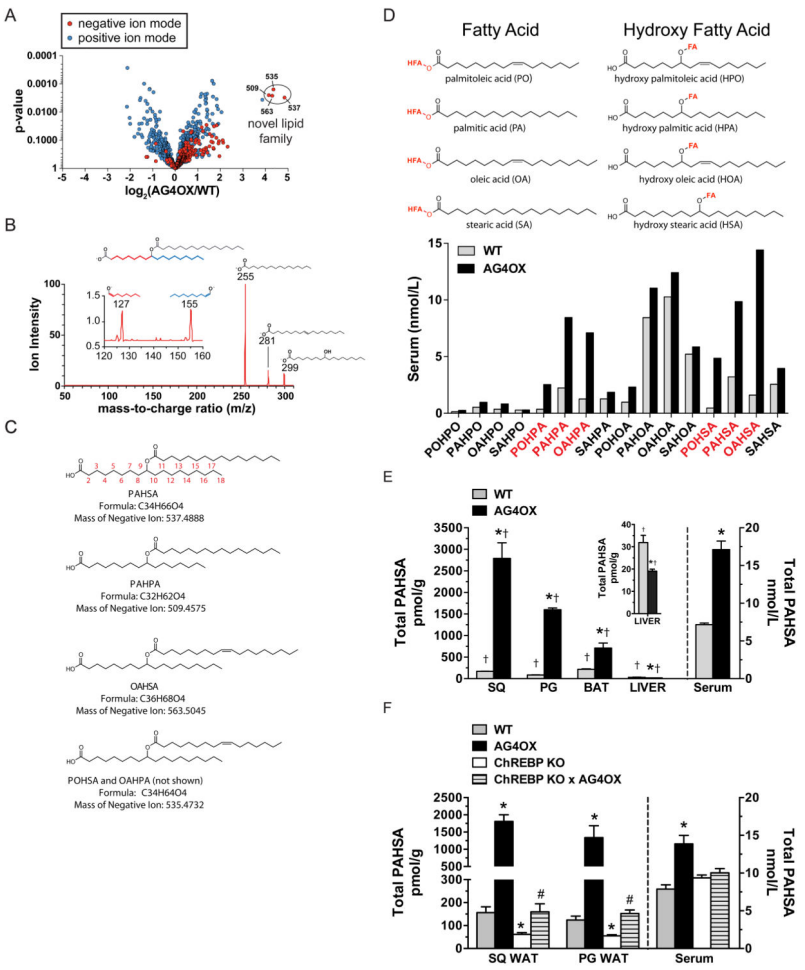

Figure 1. Discovery and characterization of a class of lipids (FAHFAs)

A) Comparative lipidomics of SQ white adipose tissue (WAT) from AG4OX and WT mice reveals the presence of a group of ions at m/z 509 (PAHPA), 535 (POHSA/OAHPA), 563 (OAHSA) and 537 (PAHSA) that are elevated 16–18-fold in AG4OX mice. B) Structural analysis of the 537 ion from AG4OX WAT by tandem MS demonstrates that it is composed of palmitic acid (m/z 255) and hydroxy stearic acid (m/z 299). Octadecanoic acid (m/z 281) results from the dehydration of hydroxy stearic acid. Fragmentation at high collision energies produces two ions at m/z 127 and 155, identifying carbon 9 as the position of the hydroxyl group on hydroxy-stearic acid, confirming the structure to be 9-PAHSA. C) Acyl chain carbon numbering scheme, molecular formula, mass and names of FAHFAs from the m/z 537 (PAHSA), m/z 509 (PAHPA), m/z 563 (OAHSA) m/z 535 (POHSA or OAHPA) ions. D) Constituent fatty acid and hydroxy-fatty acid components of FAHFAs. Quantification of 16 FAHFA family members identified in serum of WT and AG4OX mice. E) Total PAHSA levels in serum and tissues of WT and AG4OX mice. Inset, liver total PAHSA levels. n=3–5/group, *p<0.05 versus WT (t-test), †p<0.05 versus all other tissues within the same genotype (ANOVA). F) Total PAHSA levels in SQ-WAT, PG-WAT and serum of WT, AG4OX, ChREBP KO and AG4OX/ChREBP KO mice. n=3–5/group,

*p<0.05 versus all other genotypes within same tissue or serum (ANOVA), # p<0.05 versus AG4OX and ChREBP-KO. Data are means±sem.

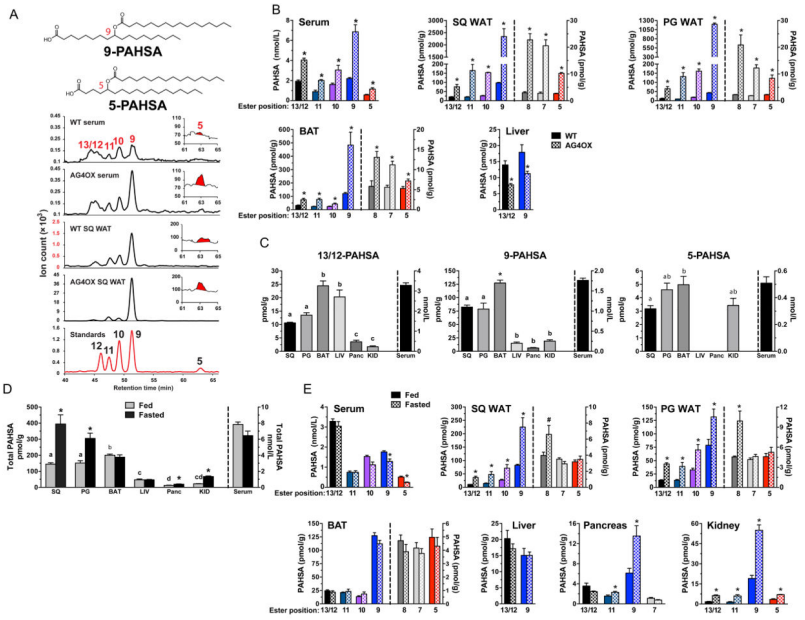

Figure 2. Identification and quantification of PAHSA isomers in mouse serum and tissues

A) Co-elution of PAHSA isomers from serum and SQ WAT of WT and AG4OX mice with synthetic standards for individual PAHSA isomers. The peak for 5-PAHSA is shown in red in the inset. B) Distribution and quantification of PAHSA isomers in serum and tissues of WT and AG4OX mice. 'Ester position' refers to the location of the ester bond in PAHSA isomers. n=3–5/group, *p<0.05 versus WT (t-test). C) Distribution and quantification of 13/12-, 9- and 5-PAHSA isomers in serum and tissues of WT female FVB mice. n=3–5/group, [a,b,c] Tissues with different letters are different from each other within the same isomer panel (p<0.05, ANOVA). D) Total PAHSA levels and E) PAHSA isomer levels in serum and tissues of WT mice in fed or fasted (16 h) states. *p<0.05 versus fed (t-test). 'Ester position' refers to the location of the ester bond in PAHSA isomers. n=3–5/group, *p<0.05, #<0.07 versus fed (t-test) [a,b,c,d]Tissues with different letters are different from each other for the fed state (p<0.05, ANOVA). Data are means±sem. See also figure S1.

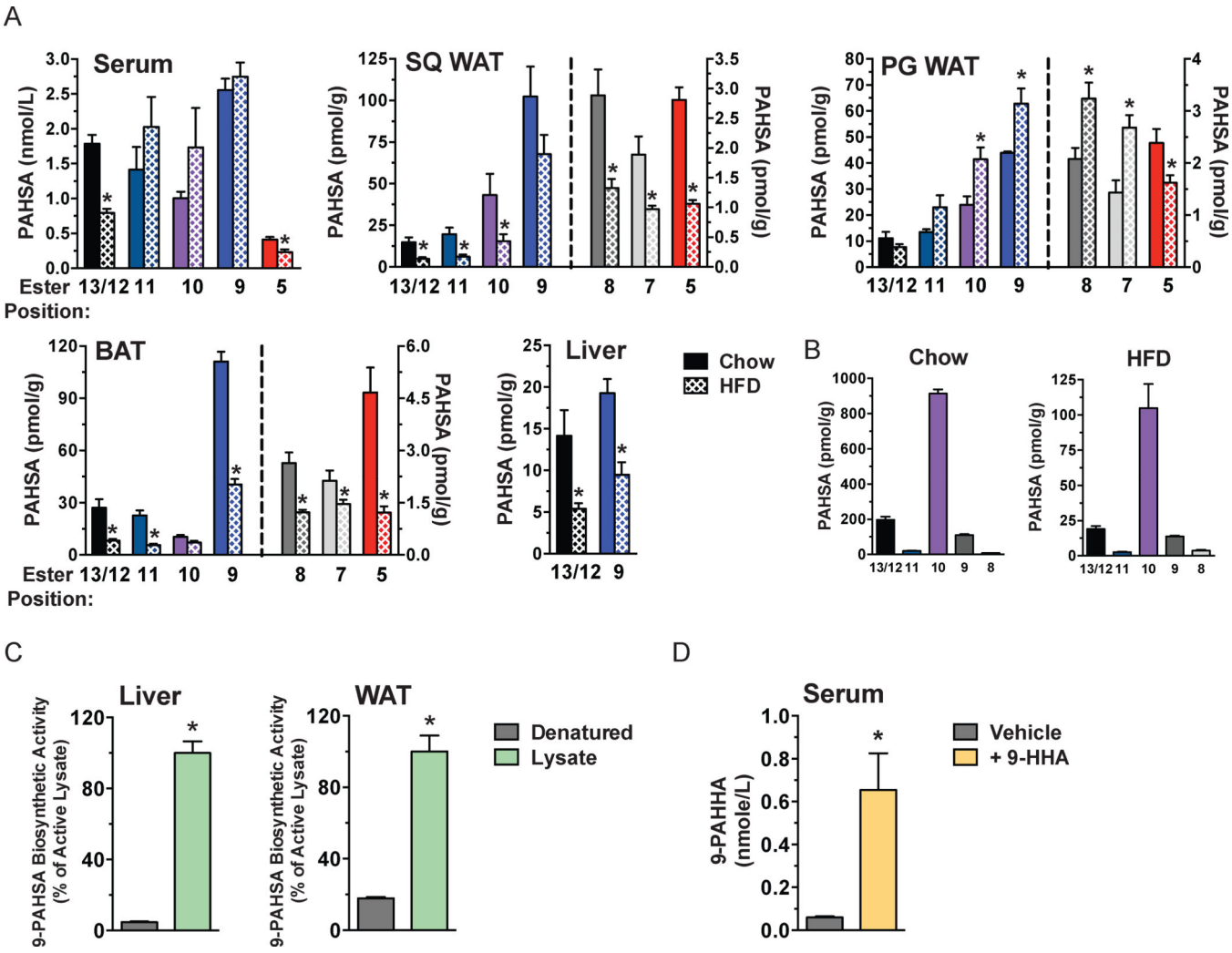

Figure 3. PAHSA isomer levels in tissues and food of mice on chow or HFD and biosynthetic activity of PAHSAs in liver, WAT and serum

A) Quantification of PAHSA isomers in serum, SQ WAT, PG WAT, BAT and liver of WT female FVB mice fed on chow or HFD for 9 weeks. 'Ester position' refers to the location of the ester bond in PAHSA isomers. n=3–6/group, *p<0.05 versus chow (t-test). B) Quantification of PAHSA isomers in mouse chow and HFD. n=3/group. C) 9-PAHSA levels in liver and PG-WAT lysates incubated with palmitoyl-CoA and 9-hydroxy stearic acid and heat-denatured Controls. n=3/group, *p<0.05 versus heat-denatured Controls (t-test). D) 9-palmitic-acid-hydroxy-heptadecanoic-acid (9-PAHHA) serum levels in mice 3h post gavage with 9-hydroxy-heptadecanoic-acid (9-HHA) or vehicle control. n=3/group, *p<0.05 versus vehicle (t-test). Data are means±sem. See also figure S2.

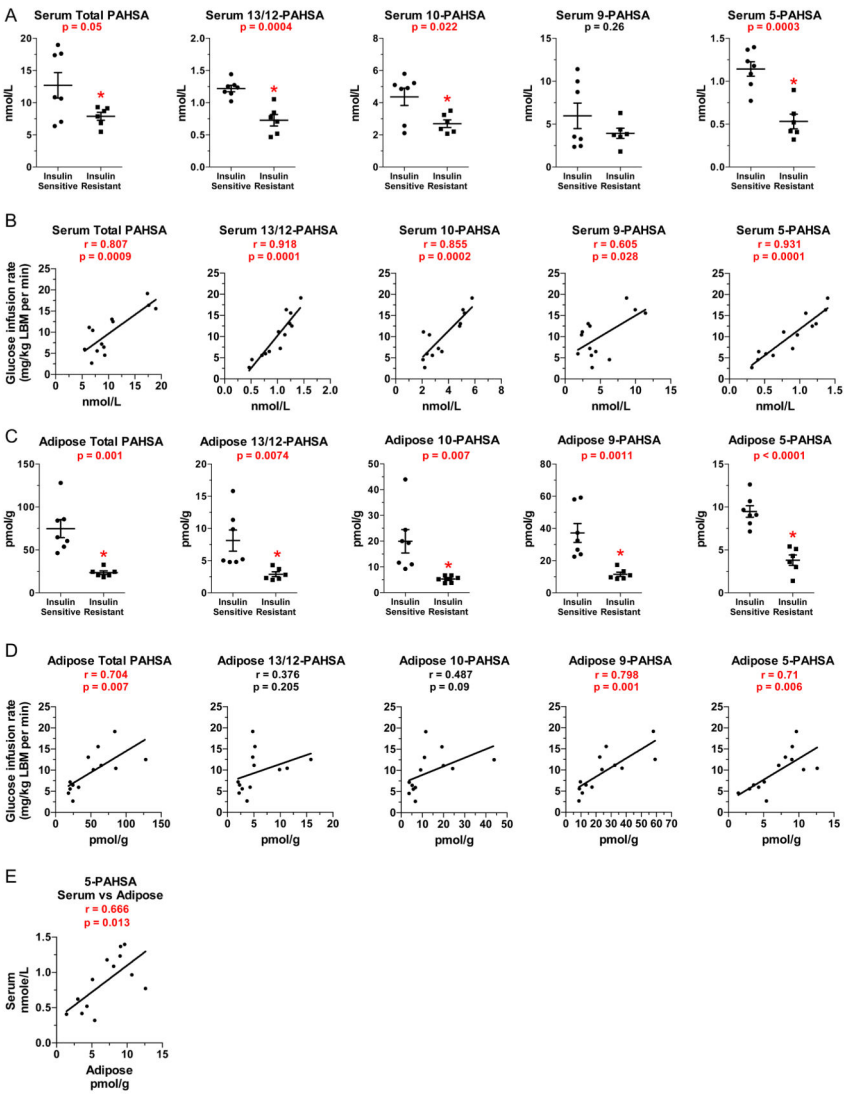

Figure 4. PAHSA levels are decreased in insulin-resistant humans and levels correlate with insulin sensitivity

A) Quantification of total PAHSAs and individual PAHSA isomers in serum of insulin-sensitive and insulin-resistant nondiabetic humans (see table S2 for metabolic characteristics). n=6–7/group. B) Correlation between insulin-sensitivity (clamp glucose infusion rate) and serum total PAHSA and individual PAHSA isomers. n=13. C) Quantification of total PAHSA and individual PAHSA isomers in SQ WAT of insulin-sensitive and insulin-resistant humans. n=6–7/group. D) Correlation between insulin-sensitivity (clamp glucose infusion rate) and SQ WAT total PAHSA and individual PAHSA isomers. n=13. E) Correlation between SQ WAT and serum 5-PAHSA levels. LBM: lean body mass. Individual p-values are shown on graphs, *p<0.05 versus insulin-sensitive (t-test, panels A and C). Data are means±sem for panels A and C. Correlations were determined by linear regression analysis for Panels B, D and E.

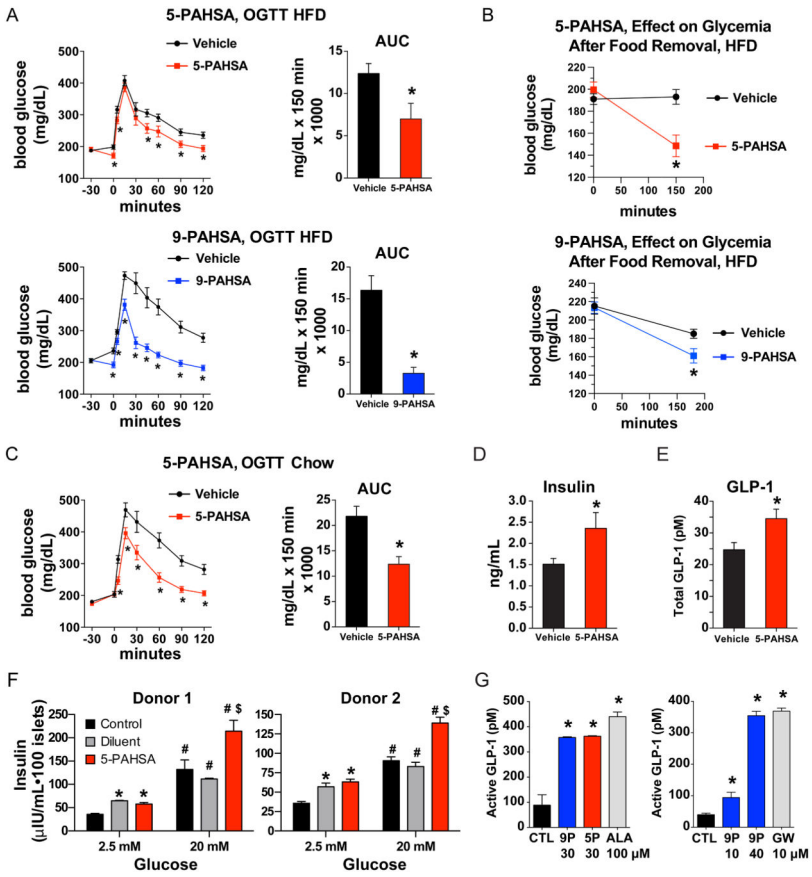

Figure 5. PAHSAs improve glucose tolerance and ambient glycemia *in vivo* and augment insulin and GLP-1 secretion

A) 4.5 hours after food removal, HFD-fed mice were gavaged with 5-PAHSA (upper panel), 9-PAHSA (lower panel) or vehicle control. 30 min later an oral glucose tolerance test (OGTT) was performed. n=12–14/group, mice were on HFD for 42–52 weeks. *p<0.05 versus vehicle at same time (t-test). Area under the curve (AUC) was calculated from-30 to 120 min. *p<0.05 versus vehicle (t-test). B) 2.5 hours after food removal, HFD-fed mice were gavaged with 5-PAHSA (upper panel), 9-PAHSA (lower panel) or vehicle control. Glycemia was measured immediately before (time 0) and at 2.5 hours (5-PAHSA) or 3 hours (9-PAHSA) after PAHSA gavage. n=12–14/group. *p<0.05 versus vehicle (t-test). C) 4.5 hours after food removal, aged, chow-fed mice (45-weeks old) were gavaged with 5-PAHSA 30 min prior to an OGTT. n=12–14/group. *p<0.05 versus vehicle at same time (t-test). Area under the curve (AUC) was calculated from−30 to 120 min. *p<0.05 versus vehicle (t-test). D) Serum insulin levels and E) serum GLP-1 levels 5 min post glucose challenge in chow-fed mice gavaged with 5-PAHSA or vehicle (glucose values shown in panel C). n=12–14/group, *p<0.05 versus vehicle (t-test). F) Insulin secretion from primary human islets from two independent donors. Islets were incubated with low (2.5 mM) or high (20 mM) glucose *ex vivo* in the presence of 5-PAHSA (20 μM) or Control (KRB buffer). Diluent for 5-PAHSA was methanol (0.25%) in panel F. n=100 islets/condition, *p<0.05 versus control 2.5 mM glucose (t-test), #p<0.05 versus all treatments at 2.5 mM glucose (t-test), $p<0.05 versus control and diluent at 20 mM glucose (t-test). G) Active GLP-1

secretion from STC-1 cells in response to 5-PAHSA (5-P), 9-PAHSA (9P), α-Linolenic Acid (ALA), GW9508 (GW) or vehicle control (CTL, DMSO). n=4/group, *p<0.05 versus vehicle (CTL) (t-test). Data are means±sem. See also table S3 and figure S3.

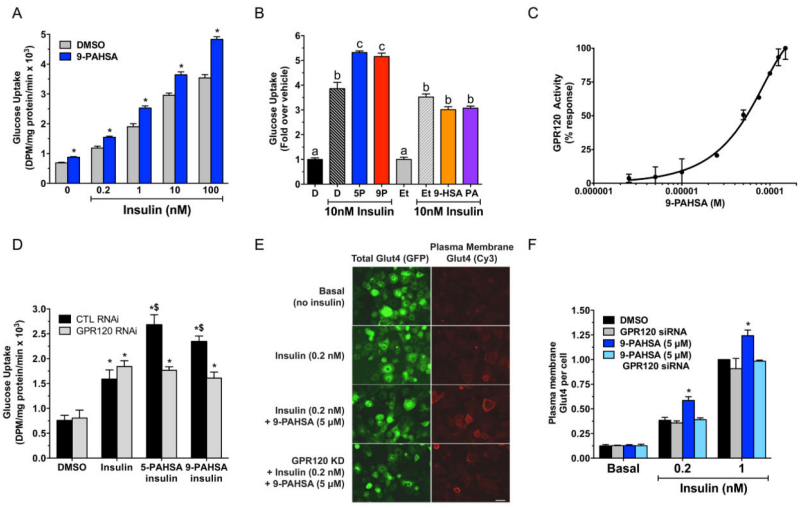

Figure 6. PAHSAs regulate glucose uptake and Glut4 translocation via GPR120

A) Insulin–stimulated glucose transport in 3T3-L1 adipocytes treated with 9-PAHSA (20μM) or vehicle (DMSO) control for 6 days. n=6/group, *p<0.001 versus vehicle (DMSO) at the same insulin concentration (ANOVA). B) Glucose transport in 3T3-L1 adipocytes treated for 48h with 9-PAHSA, 5-PAHSA, palmitic acid (PA), 9-hydroxy stearic acid (HSA) at 20μM or their respective vehicle controls (DMSO for 9- and 5-PAHSA. Ethanol for PA and HSA). n=6/group. ^{a,b,c}groups with different letters are different from each other p<0.05 (ANOVA). C) Dose response of 9-PAHSA on GPR120 binding and receptor activation. n=3 wells/condition. D) Insulin (10nM)–stimulated glucose transport in 3T3-L1 adipocytes transfected with control siRNA (CTL) or GPR120 siRNA and treated with 5-PAHSA (10μM), 9-PAHSA (10μM) or vehicle (DMSO) control for 2 days. n=3/group, *p<0.05 versus control siRNA or GPR120 siRNA with DMSO without insulin (ANOVA), $^{\$}$p<0.05 versus all other conditions except each other (ANOVA). E) Glut4 plasma membrane translocation in 3T3-L1 adipocytes transfected with control siRNA or GPR120 siRNA and treated with 9-PAHSA in the presence or absence of insulin. Scale bar=50 micrometers. F) Quantification of Glut4 translocation in panel E. Bars show means of 6 independent experiments without siRNA knockdown and 3 with siRNA knockdown. Each experiment had an n>50 cells/condition.*p<0.05 versus everything else at same insulin concentration (ANOVA). All data are means±sem. See also figure S4.

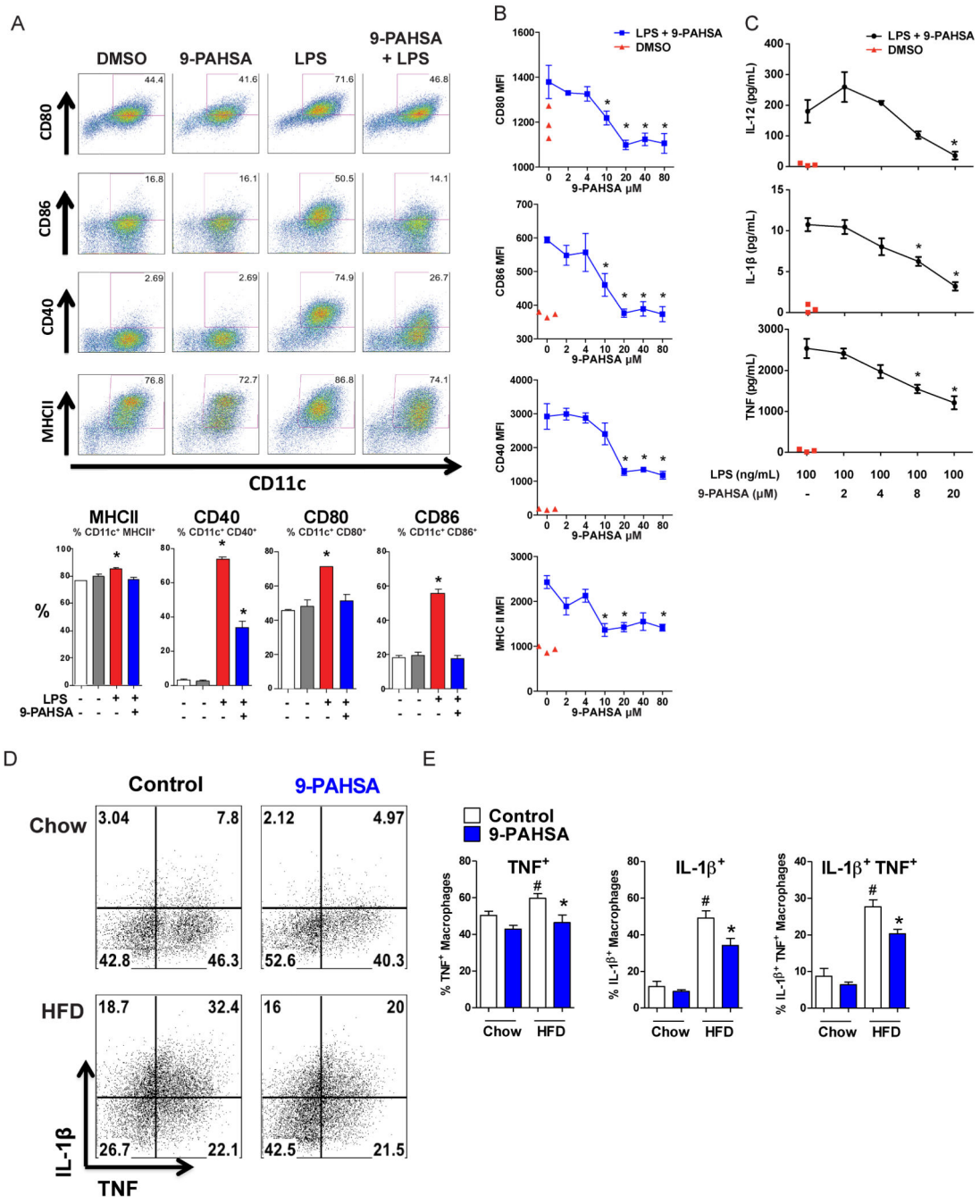

Figure 7. 9-PAHSA inhibits LPS-induced dendritic cell maturation *in vitro* and pro-inflammatory cytokine production from adipose tissue macrophages *in vivo*

A) LPS induces dendritic cell (DC) maturation (increased percentage of $CD11c^+$ cells expressing co-stimulatory molecules, CD80, CD86, CD40, and MHCII). This LPS effect is reduced in the presence of 9-PAHSA (40 μM) compared to vehicle (DMSO) control. Quantification of $CD11c^+$ cells which are positive for co-stimulatory molecules from the panel above. n=3 mice/group. B) LPS–induced DC maturation is inhibited by increasing concentrations of 9-PAHSA. Red triangles represent vehicle for 9-PAHSA (DMSO) without LPS. MFI: median fluorescence intensity. n=3 mice/group, C) LPS–induced cytokine

secretion from DC's is inhibited by increasing concentrations of 9-PAHSA compared to vehicle for 9-PAHSA (DMSO, '-') control. Red triangles represent vehicle for 9-PAHSA (DMSO, '-') without LPS. n=3 mice/group. D) Flow cytometry representation of AT macrophages expressing TNFα and IL-1β. Mice fed on HFD or chow mice were gavaged for 3 days with 9-PAHSA (30mg/kg for chow mice and 45mg/kg for HFD mice) or vehicle control. PG-WAT was harvested on day 4 and the stromal vascular cells were incubated in vitro with PMA, ionomycin and brefeldin for 5 hours. AT macrophages ($CD45^+CD11b^+F4/80^+$) were stained intracellularly for TNFα and IL-1β. E) Quantification of panel D percentage of AT macrophages expressing TNFα, IL-1β or both. n=5 mice/group. LPS concentration is 100ng/ml for all panels. *$p<0.05$ versus LPS-activated cells without PAHSA treatment (A-C) or control cells, same diet (E) by one-way (A-C) and two-way ANOVA (D). $^{\#}p<0.05$ versus all other groups by two-way ANOVA. Data are means ±sem. See also figure S5.